ABS Polymer Electroless Plating through a One-Step Poly(acrylic acid) Covalent Grafting

Alexandre Garcia,*,† Thomas Berthelot,† Pascal Viel,† Alice Mesnage,† Pascale Jégou,† Fabien Nekelson,‡ Sébastien Roussel,‡ and Serge Palacin†

CEA, IRAMIS, LSI Irradiated Polymers Grp (UMR 7642 CEA/CNRS/Ecole Polytechnique), F-91128 Palaiseau Cedex and CEA, IRAMIS, SPCSI Chemistry of Surfaces and Interfaces Grp, F-91191, Gif-sur-Yvette, France, and Pegastech, 86 rue de Paris, Bât. Erables, F-91400 Orsay, France

ABSTRACT A new, efficient, palladium- and chromium-free process for the electroless plating of acrylonitrile-butadiene-styrene (ABS) polymers has been developed. The process is based on the ion-exchange properties of poly(acrylic acid) (PAA) chemically grafted onto ABS via a simple and one-step method that prevents using classical surface conditioning. Hence, ABS electroless plating can be obtained in three steps, namely: (i) the grafting of PAA onto ABS, (ii) the copper Cu^0 seeding of the ABS surface, and (iii) the nickel or copper metallization using commercial-like electroless plating bath. IR, XPS, and SEM were used to characterize each step of the process, and the Cu loading was quantified by atomic absorption spectroscopy. This process successfully compares with the commercial one based on chromic acid etching and palladium-based seed layer, because the final metallic layer showed excellent adhesion with the ABS substrate.

KEYWORDS: electroless • poly(acrylic acid) grafting • ABS • copper seed layer • chromium and palladium free

1. INTRODUCTION

Metallization of plastics is widely used today in various technological applications ranging from the fabrication of printed circuits in microelectronics to decorative coatings in general manufacturing. Through metallization, the specific properties of plastics, such as light weight, design flexibility, and low cost of manufacturing, are enriched by the addition of properties usually associated with metals. These include reflectivity, abrasion resistance, electrical conductivity, and a variety of decorative effects. The processes that can be used for metallizing plastics (1, 2) can be either in gaseous phase such as physical (3) and chemical (4) vapor deposition or in solution as in wet-chemical metallization, i.e., plating (5). Plating can be subdivided into electroless plating and electroplating (6, 7).

Electroless metal plating is the most used method. Common process involves three main steps: (i) the surface preparation, (ii) the surface activation or surface seeding with the metal that is the catalyst of the next step, (iii) the electroless plating bath, which consists of a redox reaction between metallic ions (Ni^{2+} or Cu^{2+}) and a strong reducer both contained in the same solution. To activate the metal reduction onto the polymer, noble metal Pd is usually employed as catalyst to initiate the electroless plating (8−10). The development of Pd-free catalysts as a means of the cost and environment footprint of the plating process has been increased. Au or Ag nanoparticles are well-known electroless catalysts and can substitute for Pd in this role (11, 12). However, recently, the use of Cu and Ni species has spurred interest in the development of catalysts derived from less expensive metals (10, 13−19). Nevertheless, whatever the catalyst, the main difficulty of this process consists of chemisorbing the catalyst as metallic particles on the polymer surface. Several routes have been proposed in the literature for this purpose depending on the polymer and the targeted properties (13, 19−24). Indeed, various types of plastics can be plated, including acrylonitrile-butadiene-styrene (ABS) polymers, which are among the most widely used polymers in industry because of their excellent toughness, good dimensional stability, good processability, chemical resistance, and low cost (25−27). Plating ABS with an adherent metal layer is only possible if an appropriate etchant system is previously employed for surface conditioning in order to improve the adhesion and the surface seeding of the electroless catalyst. Up to now, the best method is based on a chromic acid etching, which aims to increase the surface energy and wettability of ABS plastics by oxidizing its surface (28). Moreover, chromic acid dissolves the polybutadiene nodes in ABS, which increases the surface roughness and significantly improves the mechanical adhesion. However, because of the future European ban on chromium wastes, that efficient process needs to be replaced (29, 30). Numerous chromium-free etchings in solution (15, 31) and dried techniques, such as ion-assisted laser treatment (32), plasma modification (33), and excimer UV laser (34) have been developed but they are neither as efficient as chromic acid etching for reaching sufficient adhesion, nor available on the industrial scale. Taking into account that the cost of palladium, as the catalyst of the second step of the process, has increased in recent years, the current electroless plating method is likely to become more and more expensive.

* Corresponding author. E-mail: alexandre.garcia@cea.fr. Phone: 00 33 1 69 08 12 80.

Received for review January 7, 2010 and accepted March 10, 2010

† CEA.

‡ Pegastech.

DOI: 10.1021/am1000163

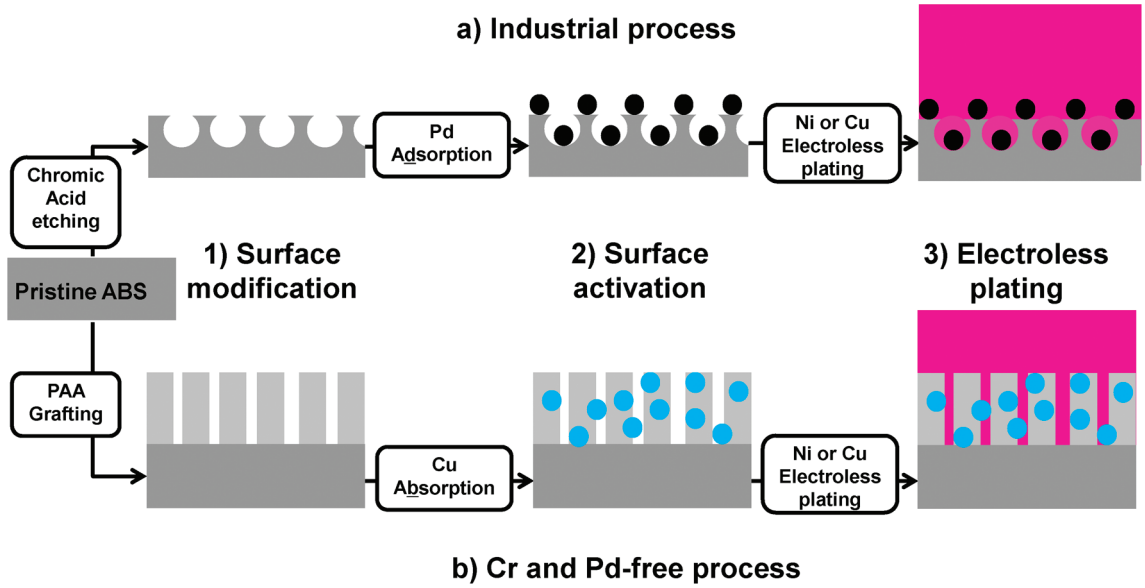

FIGURE 1. Surface preparation of ABS substrates for electroless metallization by (a) the usual industrial process and (b) our Cr- and Pd-free process.

To overcome these limitations, a chromium-free efficient process for electroless metallization on various polymers, also avoiding palladium as catalyst has been developed and is described in this paper. That new process is essentially based on the formation of a robust interphase between the plastics surface and the metal layer, which is intended to replace the rough interface that usually results from the chromic acid treatment. Indeed, that rough interface both promotes the transient deposition of catalytic particles, thanks to polar chemical groups formed upon the plastics oxidation, and increases the final adhesion between the plastics and the final metal layer, thanks to the interdigitation between the two materials. A bonded interphase should exhibit similar properties, thanks to specific affinity for the catalyst, robust anchoring on the plastics surface, and deep interpenetration with the metal layer. We will also evaluate the replacement of the classical palladium-based catalyst by copper nanoparticles formed in situ by reduction of copper(II) ions.

Recent works (10, 35−37) have demonstrated that the grafting of complexing groups on various substrates (gold, silica, polyimide) may allow satisfactory metallization, but these processes are inappropriate for ABS, the most widely electroless plated plastics. In our case, the interphase will be a thin polymer film (poly(acrylic acid), PAA) truly grafted on the ABS surface using a new grafting technology named GraftFast developed in the Laboratory of Chemistry of Surfaces and Interfaces (38, 39). It consists of a short one-step reaction occurring at atmospheric pressure, from aqueous solutions, which leads to stable, homogeneous and covalently coated PAA thin polymer film. Mevellec et al. (40) have thoroughly described the method, which proceeds via a "grafting to" mechanism with most vinylic monomers such as acrylic acid (AA) onto various substrates like metals (Au, Zn, Ti), glasses, carbon, or PTFE. In all cases, the first grafting layer and the initiation of radical polymerization are obtained via the redox activation of various aryl diazonium salts, synthesized in situ from the corresponding aryl amines. Thus, carboxylate groups contained in grafted PAA, at suitable pH, may act as complexing sites to immobilize Cu^{2+} ions. We demonstrate here that, once reduced by a suitable reducing agent, Cu^0 particles formed in situ from PAA-immobilized Cu^{2+} ions can be successfully used as metallization catalyst for the electroless metal deposition on ABS. Moreover, thanks to the metallic cations entanglement into grafted PAA acids chains, mechanical anchoring of the final metallic layer is also obtained by this process.

2. EXPERIMENTAL SECTION

Materials. ABS of technical quality was obtained from Pegastech as common test samples used in the industrial field. 1-4-Diaminophenylene dihydrochloride (Fluka, ≥99%), acrylic acid (Sigma Aldrich, ≥99%), sodium nitrite (Fluka, ≥99%) and iron powder (Prolabo VWR, 98%) were used for the poly(acrylic acid) grafting using the GraftFast technology. Cupric sulfate $CuSO_4 \cdot 5H_2O$ (Fluka, ≥99%), and sodium borohydride powder (Sigma Aldrich, ≥98.5%) were used for the copper chelation and reduction. Then, for the electroless metal deposition, two baths were used: The first one was an industrial nickel plating bath (NipositTM PM 988 supplied by Rohm and Hass) and the second plating bath was a homemade copper plating bath with a copper salt $CuSO_4,5H_2O$ (Fluka, ≥99%), formaldehyde (Sigma Aldrich, 37 wt % solution in water) and disodium tartrate $C_4H_4Na_2O_6 \cdot 2H_2O$ (Merck, ≥ 99.5%). The classical industrial conditioning step was reproduced using chromium(VI) oxide CrO_3 (Sigma Aldrich, ≥98%) for the chromium acid etching, stannous chloride $SnCl_2,2H_2O$ (Sigma Aldrich, ≥99.99%) for the sensitization solution and palladium chloride (Sigma Aldrich, ≥99.9%) for the activation solution. The electroless plating was carried out with the homemade copper plating bath previously described (41). Lastly, PAA spin-coating onto ABS substrates has been carried out using poly(acrylic acid) (Sigma Aldrich, average $M_w \approx 2000$).

Electroless Metal Deposition Process. The electroless plating process described in this work is divided into three main steps as shown in Figure 1.

Surface Modification Step: Covalent Grafting of Poly(acrylic acid) on ABS Surfaces. In a typical experiment, 1-4-

phenylenediammonium dihydrochloride was dissolved in a 0.5 M HCl solution to obtain 100 mL at 0.1 M (solution 1). Under stirring, 15 mL of $NaNO_2$ (0.1 M) was added stepwise to 15 mL of solution 1 in order to synthesize the aryldiazonium salt. Acrylic acid (15 mL) was then introduced into this solution. ABS substrates ($4 \times 1 \times 0.2$ cm^3) were introduced in the beaker, and iron powder (2.25 g) was added to the solution. After immersion for 2 h at 38 °C, ABS substrates were sonicated twice for 10 min in alkaline solution (NaOH, 1 M) and deionized water. The rinsing treatment allowed discarding most of the physisorbed matter.

Surface Activation Step: Chelation and Reduction of Metallic Cations. PAA-modified ABS substrates were immersed during 10 min into an alkaline (NH_3, 0.6 M) copper sulfate $CuSO_4 \cdot 5H_2O$ (0.1 M) solution at room temperature to induce an ion-exchange process. Afterward, samples were rinsed with deionized water. In order to reduce Cu^{2+} ions previously chelated by the carboxylate groups contained in grafted PAA films, modified ABS substrates were immersed into a sodium borohydride ($NaBH_4$)—NaOH (0.1 M) solution at 40 °C for 10 min.

Metallization Step: Electroless Metal Deposition Bath. The surface-activated ABS substrates were finally placed in the electroless metal plating baths. Two plating baths were tested. The first one was a proprietary nickel plating bath (NipositTM PM 988) of complex and unknown composition. Sodium hypophosphite NaH_2PO_2,H_2O was the reducing agent, optimum conditions were obtained with a nickel content of 4 g L^{-1}, a $NaH_2PO_2 \cdot H_2O$/Ni ratio of 3.75, and a pH equal to 9,4 and gave a final Ni coating containing 4—8% of phosphorus. ABS substrates were left in the bath for 10 min at 34 °C.

For the second case, a homemade electroless copper plating bath was used which contained $CuSO_4 \cdot 5H_2O$ as a source of Cu^{2+} ions (10 g L^{-1}), NaOH (12 g L^{-1}), disodium tartrate (18 g L^{-1}) as complexing agent, and formaldehyde (10 mL.L^{-1}) as a reducing agent, with a pH equal to 12.4. ABS substrates were left in the bath for 10 min at 40 °C (41).

"Industrial" Process: Chromic Acid Etching and Palladium Seed Layer Deposition. The industrial process was reproduced by mixing two different published works: First, the chromic acid etching step was based on a classical method described in Mallory's book (7). Second, the sensitization and activation step were based on the process described by Jiang et al. (8). Once activated by the palladium particles, the ABS substrates were plated with copper following the same method than in the case of the Cr- and Pd-free process.

3. CHARACTERIZATION

Spectroscopic Methods. Infrared spectra were recorded on a Bruker Vertex 70 spectrometer equipped with an Attenuated Total Reflection (ATR) Pike-Miracle accessory. The detector was a MCT working at liquid nitrogen temperature. The spectra were obtained after 256 scans at 2 cm^{-1} resolution.

XPS studies were performed with a KRATOS Axis Ultra DLD spectrometer, using the monochromatized Al Kα line at 1486.6 eV. The pass energy of the analyzer was kept constant at 20 eV for C_{1s} core level scans. The photoelectron takeoff angle was 90° with respect to the sample plane, which provides an integrated sampling probe depth of ca. 15 nm.

Atomic absorption spectroscopy was carried out on a Thermo Fisher Scientific Atomic Absorption Spectrometer (ICE 3000 Series) with a hollow cathode lamp for Co—Cu—Mn—Ni at a primary wavelenght of 324.8 nm and a bandpass of 0.5 nm using an air—acetylene flame at a gaz flow rate of 0.9 L/min and a 10 wt % HNO_3/deionized water matrix. The lamp current was 7.5 mA.

The scanning electron microscopy images were recorded by a Hitachi S4800 equipped with a field-emission gun (FEG-SEM) and coupled with an energy dispersive X-ray spectrometer (EDX).

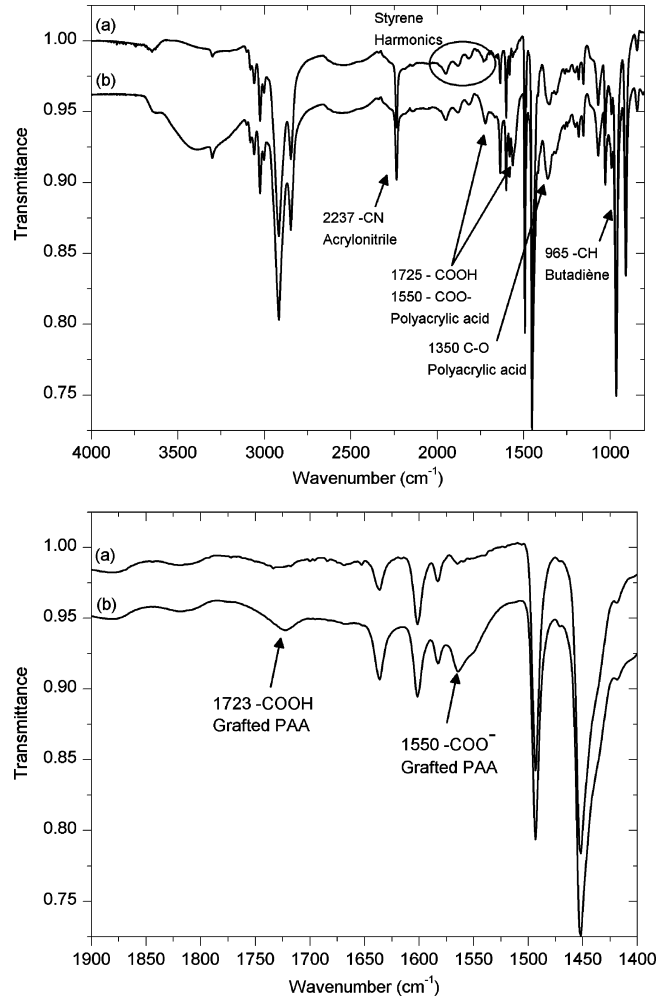

FIGURE 2. IR-ATR spectra of ABS substrate (a) before and (b) after PAA grafting with a close-up of the carboxylic acid characteristic bands (bottom).

Four-point probe (S302K-LRM, Lucas Lab) was used to measure the resistivity of the electrolessly deposited copper layers.

Mechanical Adhesion Test. The mechanical adhesion between the metallic layer and the ABS substrates was studied by a qualitative Scotch tape test inspired by the standard ASTM D3359 Scotch tape test (cross-cut tape test). It consists of sticking a high-performance transparent scotch-tape (Progress) onto the squared metallized ABS and then to remove it suddenly. Although qualitative, that well-used test allows for direct comparison of the adhesion of films obtained under various conditions on similar substrates.

4. RESULTS AND DISCUSSIONS

Covalent Grafting of Poly(acrylic acid) on ABS Surfaces. Poly(acrylic acid) has been grafted onto ABS substrates via the GraftFast technology, which is a concerted aryldiazonium reduction and AA polymerization (see the Supporting Information for details). Mevellec et al. (40) already pointed out the covalent grafting of PAA on various surfaces such as metals, glass, carbon nanotubes or PTFE by means of X-ray photoelectron and infrared spectroscopies. Here, we demonstrate that the process is also efficient on ABS.

First of all, in Figure 2, pristine ABS substrate was analyzed by ATR-FTIR and showed intense and characteristic absorption

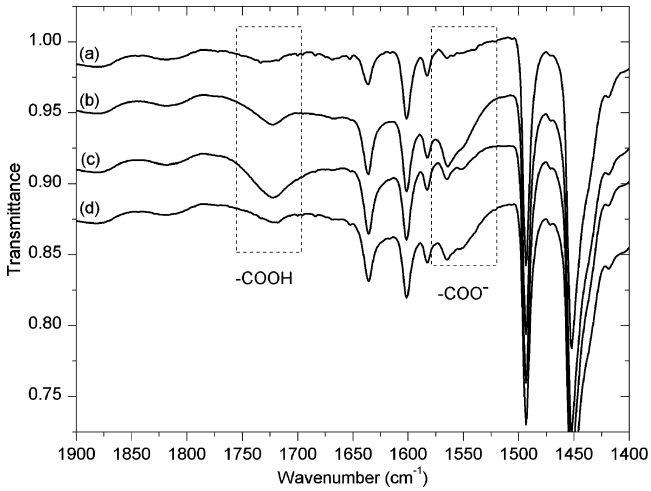

FIGURE 3. IR-ATR spectra of (a) pristine ABS, (b) after PAA grafting followed by rinsing with an alkaline solution (pH 13), (c) rinsing with an acidic solution (pH 1), and (d) after Cu^{2+} chelation.

bands at 2237, 1452, 1354, 1070, and 1028 cm^{-1} due to the acrylonitrile component of the copolymer, at 2920, 1637, 1450, 965, and 910 cm^{-1} due to the butadiene component, and at 2924, 2850, 1602, 1494, 1450, 910 cm^{-1} and all benzene harmonic absorption bands (2000−1600 cm^{-1}) due to the styrene component (42).

For PAA-grafted ABS, carboxylic group absorptions bands clearly appear either at 1723 cm^{-1} for the carboxylic acid form and/or at 1550 cm^{-1} for the carboxylate salts stretching vibrations and at 1350 cm^{-1} for the C−O stretching vibration (42). Because of the final rinsing step in deionized water (pH close to 5), the IR absorption spectra of PAA-grafted ABS generally exhibit both COOH and COO^- signals, indicating a mixed composition. Of course, the IR spectrum is dominated by the ABS absorption bands between 1500 and 1300 cm^{-1}. Figure 3 demonstrates that grafted carboxylic groups are accessible to external reagents; Indeed, immersing the PAA-grafted ABS sample successively in an alkaline and an acidic solution was followed by the expected increasing and decreasing of the carboxylate (COO^- at 1550 cm^{-1}) and carboxylic (COOH at 1725 cm^{-1}) bands, respectively.

To confirm the presence of the grafted PAA films, we studied the surfaces by XPS. Figure 4 displays XPS spectra on pristine ABS and PAA-grafted ABS surfaces. For pristine ABS, the C_{1s} core level showed one main peak centered at 285 eV, which mainly corresponds to CH and CH_2 aliphatic carbons contained in the polyacrylonitrile, polybutadiene, and polystyrene structure, and one peak at 286.8 eV, which corresponds to the CN nitrile group contained in the polyacrylonitrile component. Lastly, the polystyrene shakeup was observed around 292 eV (43). In the PAA-grafted case, in addition to the previous described peaks, a peak at 289 eV characteristic of a COOH carboxylic group was clearly observed. Moreover, according to the XPS analysis (Table 1), the CH/CN ratio increased after PAA grafting due to the contribution of CH bonds contained in the PAA film. In parallel, the O/C ratio increased 10 times and the N/C ratio decreased (5 times) after surface modification, which confirms the grafting of an oxygen-rich species. Because of the

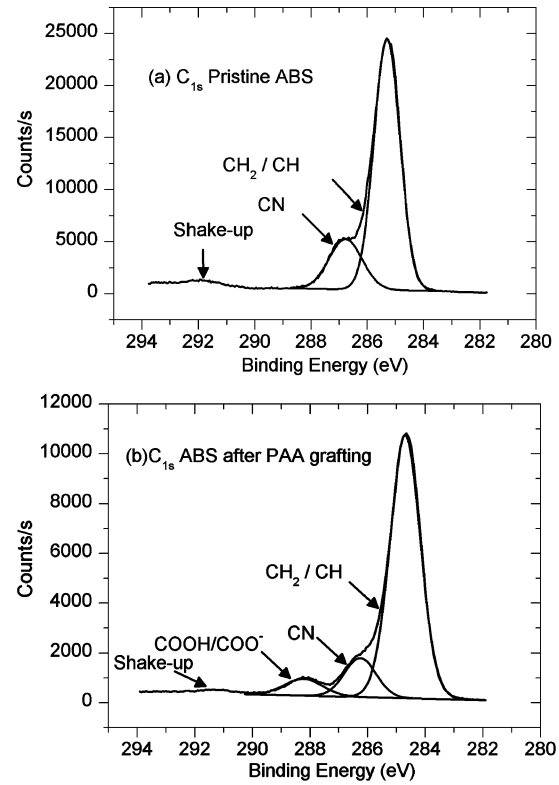

FIGURE 4. C_{1s} XPS Spectra of (a) pristine ABS and (b) PAA-grafted ABS.

Table 1. C_{1s} Normalized Atomic Ratio after PAA Grafting and Copper Complexation

	pristine ABS	ABS after PAA grafting	ABS after Cu^{2+} complexation
C1s	1.00	1.00	1.00
O1s	0.03	0.29	0.17
N1s	0.1	0.02	0.02

XPS photoelectronic mean free path ($\lambda \approx 5$ nm) for carbon, the related experimentally probed depth (a few λ), and the fact that ABS components are always observed in our spectra, we estimated that the grafted PAA film thickness was less than 15 nm.

Chelation and Reduction of Metallic Cations. When immersed in an alkaline solution containing ammonia (0.6 M) and $CuSO_4,5H_2O$ (0.1 M solution), PAA undergoes an ion exchange reaction. According to Mastumura et al. (19), the amount of loaded Cu^{2+} was found to depend on the pH solution used for ion exchange. In the absence of NH_3, the equilibrium exchange reaction was achieved after a few hours, whereas at basic pH, it was obtained after a few seconds. This was checked by flame atomic absorption spectroscopy. Indeed, after an immersion time of 30 s in the alkaline solution, the ion exchange equilibrium seemed to be achieved with an amount of Cu^{2+} around $\Gamma = 1.0$ μg cm^{-2}, whereas after 10 min in the deionized water solution, the equilibrium was not achieved and the amount of Cu^{2+} was 10 times lower. As expected from the pH-switchable chelating properties of PAA, in both chelating media the copper ions were totally released from the polymer film by immersing the substrates in an acidic solution (pH 1) for 10

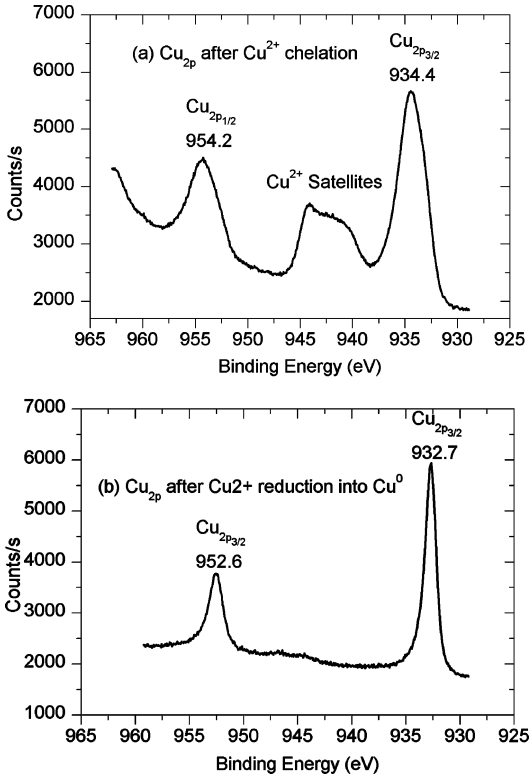

FIGURE 5. Cu_{2p} XPS spectra (a) after Cu^{2+} chelation and (b) after Cu^{2+} reduction.

min. Following the same process, various copper ions loading/unloading cycles were performed and the same amount of Cu^{2+} was obtained after each loading step, which demonstrates the full reversibility of the chelation.

The Cu^{2+} loading and the deprotonation of carboxylic acid of PAA-grafted ABS were also confirmed by infrared and XPS spectroscopies. As shown in Figure 3d, the carboxylic acid bands almost disappeared after the ion exchange, suggesting the formation of PAA−copper salts (42).

As shown in Figure 5, the Cu_{2p} spectra analysis confirmed the Cu^{2+} chelation by three peaks, respectively corresponding to $Cu_{2p3/2}$ (934.4 eV), Cu_{2p} satellites (from 938 to 945 eV), and $Cu_{2p1/2}$ (954.3 eV) core level binding energies. Besides, XPS analysis revealed a Cu/C ratio close to 2% (see the Supporting Information for details). Given that one metallic copper cation should normally be chelated by two carboxylate groups COO^- and according to the Cu_{2p}/COOH C_{1s} atomic ratio, 80% of the carboxylic groups were chelated by copper ions, which means that the PAA ion exchange properties are very efficient for copper seeding.

Reduction of Immobilized Metallic Cations. The reduction of Cu^{2+} ions immobilized by complexation in PAA-grafted ABS was then obtained by immersion of the Cu−PAA film in an alkaline solution of sodium borohydrure $NaBH_4$ and confirmed by XPS measurements with the study of the chemical state of copper. As shown in Figure 5, after immersion in $NaBH_4$, the peak of $Cu_{2p3/2}$ core level binding energy shifts partially toward lower energy and the characteristic Cu_{2p} satellites disappeared. Otherwise, the Cu/C ratio measured from XPS spectra remained constant (2%) after that reduction: all the formerly complexed copper ions were reduced within the film, without any release to the external solution.

Electroless Metal Deposition Bath. In both nickel and copper plating baths, the mechanism of the metallic ion reduction is complex and not totally understood yet (7, 44−48). However, it was shown that in the case of the nickel plating bath (Niposit TM PM 988), the Ni^{2+} reduction with hypophosphite induces some phosphorus incorporation in the metallic layer, whereas in the copper plating bath the metallic layer contains only copper.

It is noteworthy that the industrial Ni plating bath contains a stabilizer which prevents spontaneous reduction in solution (7), but may delay or even hinder the initiation of the autocatalytic reaction through a kind of poisoning of the Cu catalytic sites, hence resulting in an increase in the activation energy of the reaction (7). Thus, in the case of our copper homemade plating bath, no stabilizer was used.

Taking into account all the parameters, immersing the ABS substrate in the plating bath during 10 min allowed the formation of micrometer-thick films depending strongly on the kind of baths and the bath conditions.

The obtained metallic layers were characterized by XPS measurements and confirmed that Ni^0 and Cu^0 were successfully formed on the ABS substrates (see the Supporting Information for details).

Otherwise, based on the four-point probe method, the electrical resistivity of the as-plated copper was 3.2 $\mu\Omega$ cm, which is slightly higher than bulk copper, which is 1.67 $\mu\Omega$ cm (49). The presence of defects, hydrogen entrapment in the films, and film discontinuities are the major factors contributing to the observed increase in the resistivity of the plated films compared to that of bulk copper (50).

The metallized substrates were also observed by scanning electron microscopy and characterized by EDX measurements. As shown in Figure 6, in both cases, the metallic layer consists of 100 to 200 nm sized nanoparticles and the surface was not totally homogeneous at the microscopic scale; the metallic layer seems, however, to be more compact in the case of the copper plating bath. The electroless plating bath and more specifically the metallic growth are extremely difficult to control at the laboratory scale. Indeed, these electroless plating bath are developed for industrial production line and all the fluid mechanics involved in it. Nevertheless, the ABS section after Cu metallization showed a global homogeneous and planarized metallic top-layer and a good interfacial zone between the metal and the ABS. The metallic layer thickness is around 5−10 μm after 10 min. EDX spectra analysis revealed the presence of Cu^0 and Ni^0 and in the case of nickel deposition, phosphorus was also present and indicated a final composition of 92.5% nickel and 7.5% phosphorus ignoring carbon and oxygen residuals. EDX spectra are available on the Supporting Information.

Finally, preliminary adhesion tape tests gave very promising results: for both copper and nickel metallization, the metallic layer was fully undamaged after the tape test, as for the classical chromic acid-palladium seeding process. On

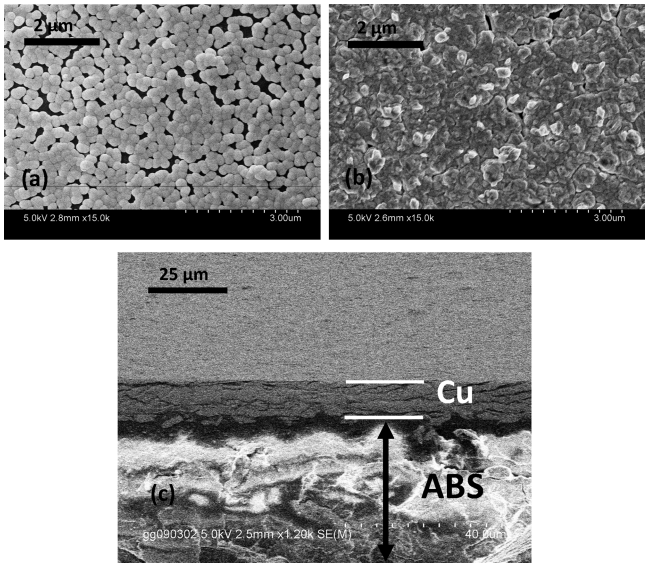

FIGURE 6. SEM images after electroless metal deposition: (a) nickel and (b) copper plating with a 2 μm scaled top view, and (c) copper plating with the 25 μm scaled ABS section with a tilt angle of 75°.

the contrary, when ABS was Cu-metallized either without any PAA grafting or after spin-coating PAA from a 0.5% w/w solution (51), the metallic layer was fully removed. That good adhesion may be attributed to the location of copper catalyst particles, which were formed in situ from complexed copper ions within the grafted PAA layer. Hence, the copper particles were buried within the PAA layer and obviously promote adhesion between the ABS substrate and the metal thin films through a nanometer-scale mechanical interlocking effect, which mimics the micrometer-scale interdigitation that occurs between the metal layer and the rough interface which results from the chromic acid treatment. Direct comparison between our process and the classical chromium-based method are currently under way in order to quantify the good mechanical adhesion reported above. Up to now, we can assume that our chromium-free process provides a promising alternative to usual chromium-based etching preparation step for the ABS electroless plating.

5. CONCLUSIONS

We have described a new and powerful method to metallize ABS plastics without the use of chromium (as etching agent) and palladium (as catalyst of the metallic layer growth). The pollutant etching step has been replaced by PAA chemical grafting using the GraftFast technology, which provides ecological benefits. Moreover, this process divided into 3 steps is cost-effective and showed a good adhesion between the final metallic layer and the ABS substrates. Further work aims at applying this process to other polymer substrates with different shapes and with quantitative adhesion tests between the metallic layer and the ABS substrates. Lastly, adaptation of this method to produce selective electroless metallization is currently under investigation.

Supporting Information Available: Chemical scheme showing mechanism of grafting; atomic absorption, XPS, and EDX data (PDF). This material is available free of charge via the Internet at http://pubs.acs.org.

REFERENCES AND NOTES

(1) Charbonnier, M.; Alami, M.; Romand, M. *J. Electrochem. Soc.* **1996**, *143*, 472–480.
(2) Sacher, E. *Metallization of Polymers 2*; Springer: New York, 2002.
(3) De Bruyn, K.; Van Stappen, M.; De Deurwaerder, H.; Rouxhet, L.; Celis, J. P. *Surf. Coat. Technol.* **2003**, *163*, 710–715.
(4) Long, D. P.; Blackburn, J. M.; Watkins, J. J. *Adv. Mater.* **2000**, *12*, 913–915.
(5) Vaskelis, A.; Norkus, H. J.; Rozovskis, G.; Vinkevicius, H. J. *Trans. Inst. Met. Finish.* **1997**, *75*, 1–3.
(6) Krulik, G. A.; Lauterer, K. R. *Modern Plastics Encyclopedia*; McGraw-Hill: New York, 1977.
(7) Mallory, G. O.; Hajdu, J. B. *ELECTROLESS PLATING: Fundamentals and Applications*; The American Electroplaters and Surface Finishers Society: Washington, D.C., 1990.
(8) Jiang, B. Q.; Xiao, L.; Hu, S. F.; Peng, J.; Zhang, H.; Wang, M. W. *Opt. Mater.* **2009**, *31*, 1532–1539.
(9) Nicolas-Debarnot, D.; Pascu, M.; Vasile, C.; Poncin-Epaillard, F. *Surf. Coating Tech.* **2006**, *200*, 4257–4265.
(10) Zabetakis, D.; Dressick, W. J. *ACS Appl. Mater. Interfaces* **2009**, *1*, 4–25.
(11) Dai, W.; Wang, W. J. *Sens. Actuators, A* **2007**, *135*, 300–307.
(12) Miyoshi, K.; Aoki, Y.; Kunitake, T.; Fujikawa, S. *Langmuir* **2008**, *24*, 4205–4208.
(13) Charbonnier, M.; Romand, A.; Goepfert, Y.; Leonard, D.; Bessueille, F.; Bouadi, A. *Thin Solid Films* **2006**, *515*, 1623–1633.
(14) Charbonnier, M.; Romand, M.; Goepfert, Y. *Surf. Coat. Technol.* **2006**, *200*, 5028–5036.
(15) Teixeira, L. A. C.; Santini, M. C. *J. Mater. Process. Technol.* **2005**, *170*, 37–41.
(16) Zhu, P. X.; Masuda, Y.; Koumoto, K. *J. Mater. Chem.* **2004**, *14*, 976–981.
(17) Hsiao, Y. S.; Whang, W. T.; Wu, S. C.; Chuang, K. R. *Thin Solid Films* **2008**, *516*, 4258–4266.
(18) Bicak, N.; Karagoz, B. *Surf. Coat. Technol.* **2008**, *202*, 1581–1587.
(19) Matsumura, Y.; Enomoto, Y.; Sugiyama, M.; Akamatsu, K.; Nawafune, H. *J. Mater. Chem.* **2008**, *18*, 5078–5082.
(20) Charbonnier, M.; Romand, M.; Goepfert, Y.; Leonard, D.; Bouadi, M. *Surf. Coating Technol.* **2006**, *200*, 5478–5486.
(21) Girginer, B.; Karagoz, B.; Urgen, M.; Bicak, N. *Surf. Coating Technol.* **2008**, *202*, 4176–4182.
(22) Rohan, J. R.; O'Riordan, G.; Boardman, J. *Appl. Surf. Sci.* **2002**, *185*, 289–297.
(23) Shibata, M.; Uda, T.; Yosomiya, T. *Thin Solid Films* **2003**, *440*, 123–128.
(24) Tang, X. J.; Bi, C. L.; Han, C. X.; Zhang, B. G. *Mater. Lett.* **2009**, *63*, 840–842.
(25) Courduvelis, C. I. *Plastics Products Design Handbook*; Marcel Dekker: New York, 1983; Vol. Part B.
(26) Harper, C. A.; Petrie, E. M. *Plastics Materials and Processes: A Concise Encyclopedia*; Wiley: Berlin, 2003.
(27) Kulich, D. M. *Kirk-Othmer Encyclopedia of Chemical Technology*, 4th ed.; Wiley: New York, 1993; Vol. 9.
(28) Wang, G. X.; Li, N.; Hu, H. L.; Yu, Y. C. *Appl. Surf. Sci.* **2006**, *253*, 480–484.
(29) EUROPEAN PARLIAMENT AND THE COUNCIL, 2002/95/EC, 2003.
(30) EUROPEAN PARLIAMENT AND THE COUNCIL, 2005/90/EC, 2006.
(31) Patel, G. N.; Bolikal, D.; Petel, H. U.S. Patent 5 160 600, 1992.
(32) Kupfer, H.; Hecht, G.; Ostwald, R. *Surf. Coat. Technol.* **1999**, *112*, 379–383.
(33) Charbonnier, M.; Romand, M. *Int. J. Adhes. Adhes.* **2003**, *23*, 277–285.
(34) Esrom, H.; Seebock, R.; Charbonnier, M.; Romand, M. *Surf. Coat. Technol.* **2000**, *125*, 19–24.
(35) Li, L.; Yan, G. P.; Wu, J. Y.; Yu, X. H.; Guo, Q. Z.; Kang, E. T. *Appl. Surf. Sci.* **2008**, *254*, 7331–7335.
(36) Liaw, W. C.; Huang, P. C.; Chen, K. P.; Chen, C. S. *Polym. J.* **2009**, *41*, 634–642.
(37) Aldakov, D.; Bonnassieux, Y.; Geffroy, B.; Palacin, S. *ACS Appl. Mater. Interfaces* **2009**, *1*, 584–589.

(38) Mévellec, V.; Roussel, S.; Tessier, L.; Chancolon, J.; Mayne-L'Hermite, M.; Deniau, G.; Viel, P.; Palacin, S. *Chem. Mater.* **2007**, *19*, 6323–6330.
(39) Mévellec, V.; Roussel, S.; Deniau, G. FR Patent 2 910 006, 2007.
(40) Mevellec, V.; Roussel, S.; Tessier, L.; Chancolon, J.; Mayne-L'Hermite, M.; Deniau, G.; Viel, P.; Palacin, S. *Chem. Mater.* **2007**, *19*, 6323–6330.
(41) Bercu, B.; Enculescu, I.; Spohr, R. *Nucl. Instrum. Methods Phys. Res., Sect. B* **2004**, *225*, 497–502.
(42) Socrates, G. *Infrared Characteristics Group Frequencies*; Wiley-Interscience: Chichester, U.K., 1994.
(43) Beamson, G.; Briggs, D. *High-Resolution XPS of Organic Polymers: The Scienta ESCA300* John Wiley & Sons: New York, 1992.
(44) Abrantes, L. M.; Correia, J. P. *J. Electrochem. Soc.* **1994**, *141*, 2356–2360.
(45) Ma, C. L.; Ye, W. C.; Shi, X. Z.; Chang, Y. L.; Chen, Y.; Wang, C. M. *Appl. Surf. Sci.* **2009**, *255*, 3713–3718.
(46) Wang, K.; Hong, L.; Liu, Z. L. *Ind. Eng. Chem. Res.* **2008**, *47*, 6517–6524.
(47) Wu, Z. J.; Ge, S. H.; Zhang, M. H.; Li, W.; Tao, K. Y. *J. Colloid Interface Sci.* **2009**, *330*, 359–366.
(48) Yin, X.; Hong, L.; Chen, B. H. *J. Phys. Chem. B* **2004**, *108*, 10919–10929.
(49) Weast, R. C. *CRC Handbook of Chemistry and Physics*; CRC Press: Boca Raton, FL, 1984.
(50) Aithal, R. K.; Yenamandra, S.; Gunasekaran, R. A.; Coane, P.; Varahramyan, K. *Mater. Chem. Phys.* **2006**, *98*, 95–102.
(51) Jackson, R. L., European Patent 0 250 867, 1988.

AM1000163